Med Mol Morphol (2006) 39:33–43
DOI 10.1007/s00795-005-0306-3


ORIGINAL PAPER

**Yu-Lan Jin · Hideaki Enzan · Naoto Kuroda
Yoshihiro Hayashi · Makoto Toi · Eriko Miyazaki
Tadashi Hamauzu · Makoto Hiroi · Li-Mei Guo
Zhe-Shi Shen · Toshiji Saibara**

# Vascularization in tissue remodeling after rat hepatic necrosis induced by dimethylnitrosamine

Received: August 23, 2005 / Accepted: November 14, 2005

**Abstract** We observed postnecrotic tissue remodeling to examine vascularization in adult rat livers. Livers, bone marrow, and peripheral blood from rats at 24 h to 14 days after an injection of dimethylnitrosamine (DMN) were examined by light microscopic, immunohistochemical, and ultrastructural methods. Numerous ED-1 (a marker for rat monocytes/macrophages)-positive round mononuclear cells infiltrated in the necrotic areas at 36 h after DMN treatment. On day 5, when necrotic tissues were removed, some of the cells were transformed from round to spindle in shape. On day 7, these cells were contacted with residual reticulin fibers and became positive for SE-1, a marker of hepatic sinusoidal endothelial cells and Tie-1, an endothelial cell-specific surface receptor, associated with frequent occurrence of ED-1/SE-1 and ED-1/Tie-1 double-positive spindle cells. Ultrastructurally, the spindle cells simultaneously showed phagocytosis and endothelial cell-like morphology. With time necrotic areas diminished, and on day 14, the necrotic tissues were almost replaced by regenerated liver tissues and thin bundles of central-to-central bridging fibrosis. Bone marrow from 12 h to day 2 showed an increase of BrdU-positive mononuclear cells. Some of them were positive for ED-1. The BrdU-labeled and ED-1-positive cells appeared as early as 12 h after DMN injection and reached a peak in number at 36 h. They were similar in structure to ED-1-positive cells in necrotic liver tissues. These findings suggest that round mononuclear ED-1-positive cells proliferate first in bone marrow after DMN treatment, reach necrotic areas of the liver through the circulation, and differentiate to sinusoidal endothelial cells. Namely, hepatic sinusoids in DMN-induced necrotic areas may partly be reorganized possibly by vasculogenesis.

**Key words** Vasculogenesis · Submassive hepatic necrosis · Dimethylnitrosamine · Macrophage · ED-1-positive stem cells

Y.L. Jin[1] · H. Enzan (✉) · N. Kuroda · Y. Hayashi · M. Toi · E. Miyazaki · T. Hamauzu · M. Hiroi · L.M. Guo · Z.S. Shen
Department of Pathology, Kochi Medical School, Kochi University, Kohasu, Oko-cho, Nankoku, Kochi 783-8505, Japan
Tel. +81-88-880-2329; Fax +81-88-880-2332
e-mail: enzanh@med.kochi-u.ac.jp

T. Saibara
Department of Gastroenterology and Hepatology, Kochi Medical School, Kochi University, Kochi, Japan

*Present address:*
[1]Department of Pathology, Affiliated Beijing Tongren Hospital, Capital University of Medical Science, Beijing, China

## Introduction

Vascularization is composed of vasculogenesis and angiogenesis.[1–3] The former is defined as the development of blood vessels derived from in situ differentiating endothelial cells, and the latter is caused by the sprouting of capillaries from preexisting vessels.[1–3] Vasculogenesis had been considered as occurring only in the early embryonic stage.[4–7] However, postnatal vasculogenesis has recently become a critical paradigm for the repair of adult ischemic myocardial tissues, hindlimb, and chorioid plexuses.[3,8–11] Pioneering work showed that endothelial progenitor cells are derived from bone marrow[3,11–16] and circulate in adult peripheral blood.[11,13,17] On the other hand, to the best of our knowledge, there have been no useful animal models for post-necrotic regeneration of the hepatic sinusoid of adult animals.

Hepatic sinusoidal endothelial cells (HSEs) are well-differentiated specific endothelial cells.[18] They possess open fenestrae that are grouped in sieve plates and lack a basal lamina.[19] Maintenance of the unique structure is prerequisite for the active metabolism of liver parenchymal cells. Because of the structural complexity and the intimate metabolic relationship with liver parenchymal cells, the HSEs are vulnerable to many kinds of liver injuries.[20–22] The injuries and regeneration of HSEs are frequently associated with those of liver parenchymal cells.

Dimethylnitrosamine (DMN), metabolized in the liver, causes a striking centrilobular necrosis accompanied by

**Table 1.** Antibodies used for immunohistochemical analysis in this study

| Antibodies | Clone | Source | Dilution | Antigen retrieval |
|---|---|---|---|---|
| Antirat hepatic sinusoidal endothelial cell | SE-1 | IBL, Japan | 5 μg/ml | 0.1% pronase E (20 min, room temperature) |
| BrdU | Bu20a | Dako, Denmark | 1/20 | 0.01 M citrate buffer (for microwave treatment, 5 min, three times) |
| Rat monocyte/macrophage | ED1 | Serotec, Oxford, England | 1/50 | 0.1% pronase E (20 min, room temperature) |
| Tie-1 | poly | Santa Cruz Biotechnology, USA | 1/50 | – |

BrdU, 5-bromo-2-deoxyuridine; –, no treatment for antigen retrieval

severe hemorrhage in many laboratory animals.[21,23,24] The aim of this study is to clarify the mechanism of vascularization after DMN-induced acute rat liver injury, using histological, immunohistochemical, and ultrastructural methods.

## Materials and methods

### Animals

Acute hepatic injury was induced by an intraperitoneal injection of DMN (Sigma, St. Louis, MO, USA) in a dose of 50 mg (diluted 1:100 with 0.15 M NaCl solution)/kg body weight in 40 male Wistar strain rats (7–10 weeks old). Five untreated rats and 5 saline-injected rats were used as normal controls. All animals were maintained under 12-h light/12-h dark cycles with food and water available ad libitum. Four rats per each group were killed at 12, 24 and 36 h and 2, 3, 5, 7, 8, 10, and 14 days after the injection. All animals were anesthetized with diethyl ether before being killed. Four rats in each time interval after DMN treatment and 3 control rats received an intraperitoneal injection of 5-bromo-2-deoxyuridine (BrdU) (10 mg/kg body weight, at a concentration of 20 mg/ml in saline) 1 h before death. This study was approved by the Animal Care and Use Committee of Kochi Medical School and followed the National Institutes of Health guidelines for humane care and use of animals.

### Examination of peripheral blood

We obtained 5-ml peripheral blood samples from all rats. Half the blood samples were measured by standard methods for red blood corpuscles (RBC, $\times 10^4/\mu l$), hemoglobin (Hb, g/dl), and white blood cells (WBC, /μl). After centrifugation (1500 rpm, 10 min), the values of serum alanine aminotransferase (ALT, IU/l) and aspartate aminotransferase (AST, IU/l) were determined. The other half was used for cytological and immunocytochemical examination. Low-density peripheral blood mononuclear cells were isolated by density centrifugation over Histopaque-1083 (Sigma). These isolated cells were fixed in 10% phosphate-buffered formalin and then embedded in paraffin using the celloidin bag method.[25]

### Light microscopy, immunohistochemistry, and double immunohistochemical stainings

Liver and bone marrow tissues obtained from DMN-treated and control groups were fixed in 10% phosphate-buffered formalin. Some of the liver frozen sections were fixed by acetone and prepared for immunohistochemical examination of Tie-1 (Santa Cruz Biotechnology, Santa Cruz, CA, USA). Some of the livers were fixed by perfusion of periodate-lysine-paraformaldehyde (PLP) solution through the portal vein for the immunohistochemical demonstration of HSEs, using a monoclonal antibody for rat HSEs (SE-1; IBL, Takasaki, Japan).[26] After perfusion, pieces of the livers were immersed in PLP solution for an additional 24 h at 4°C and then embedded in paraffin. The liver tissue sections were stained with hematoxylin and eosin, with Berlin blue method for iron, with silver impregnation for reticulin fibers, and with Azan method for collagen fibers.

Additionally, immunostaining of the liver and bone marrow tissues and peripheral blood smears was performed using the avidin-biotin-peroxidase complex (ABC) method. For visualization, each section was immersed in a substrate solution of 0.5% 3,3′-diaminobenzidine tetrahydrochloride (DAB; Sigma Chemical, St. Louis, MO, USA) as described in our previous study.[21] Antibodies employed in the present study are summarized in Table 1. For a negative control of immunostaining, the tissue sections and peripheral blood smears were incubated in normal mouse serum at the same concentration as the primary antibodies used in this study and were subsequently handled according to the same procedure as described above.

To simultaneously detect cytoplasmic ED-1, a marker for rat monocytes/macrophages,[27] and nuclear BrdU incorporation in the same sections of liver and bone marrow tissues and peripheral blood samples, double immunohistochemical stainings were applied as described in our previous study.[21] The nuclei of the cells in S phase showed a positive reaction for BrdU with brown color, and the cytoplasmic reaction product for ED-1 showed a blue color with fast blue BB.

### Double stainings using silver impregnation and ED-1 immunostaining

After silver impregnation, the sections were incubated overnight with anti-ED-1 antibody and visualized by New Fuchsin (Dako, Carpinteria, CA, USA).

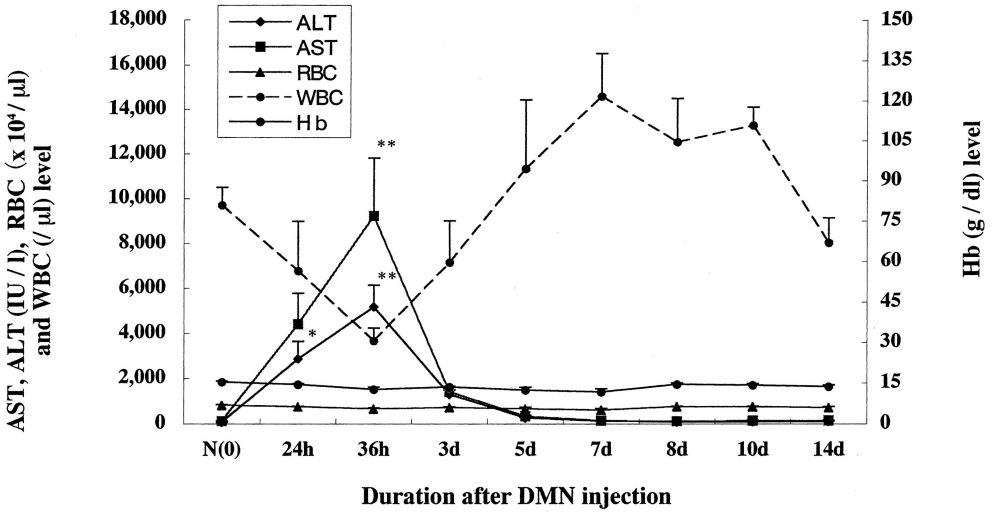


**Fig. 1.** Peripheral blood examination. The number of red blood cells (*RBC*) and the concentration of hemoglobin (*Hb*) show no significant changes throughout the experiment. The number of white blood cells (*WBC*) shows the lowest level at 36 h and then gradually increases and returns to the normal level on day 14. The values of serum aspartate aminotransferase (*AST*) and alanine aminotransferase (*ALT*) reach a peak at 36 h ($P < 0.001$) and then decrease with time. Data are expressed as mean ± SEM. *N*, normal control; DMN, dimethylnitrosamine. *$P < 0.05$, **$P < 0.001$ versus normal control

### Double immunofluorescence labelings

To clarify the relationship between the SE-1-, Tie-1-positive, and ED-1-positive cells, we carried out double immunofluorescence labelings with SE-1, Tie-1, and ED-1 antibodies in PLP-fixed paraffin sections and frozen sections. Deparaffinized sections were exposed to Alexa Fluor 594 mouse $IgG_1$ (Zenon Tricolor mouse $IgG_1$ Labeling Kit #2; Molecular Probes, Atlanta, GA, USA)-conjugated monoclonal anti-SE-1 antibody/Alexa Fluor 594 mouse $IgG_1$ (Zenon Tricolor mouse $IgG_1$ Labeling Kit #1; Molecular Probes)-conjugated monoclonal anti-ED-1 antibody for 1 h after with 0.1% pronase-E treatment as shown in Table 1. Finally, these sections were mounted with Vectashield Mounting Medium with TAPI (Vector Laboratories, Burlingame, CA, USA).

The frozen sections were incubated overnight with a polyclonal anti-Tie-1 antibody. They were incubated at room temperature for 1 h with a 1:200 dilution of biotinylated rabbit antimouse IgG $F(ab')^2$ fragment (Dako) and swine antirabbit IgG $F(ab')^2$ fragment (Dako), and then incubated at room temperature for 30 min with fluorescein isothiocyanate (FITC)-labeled streptavidin (Dako; 1:200). After washing with phosphate-buffered saline (PBS), sections were reincubated with 1% bovine serum albumin (BSA) in PBS for 30 min, and exposed to Alexa Fluor 594 mouse $IgG_1$ (Zenon Tricolor mouse $IgG_1$ Labeling Kit #2; Molecular Probes)-conjugated monoclonal anti-ED-1 antibody (AC40; Sigma; dilution 1:50) for 1 h. Finally, these sections were mounted with DAKO Fluorescent Mounting Medium (Dako).

Digital images were captured using the CoolSnap system on an Olympus BX60 microscope (Olympus America, Lake Success, NY, USA). Serial images of multistained fluorescent sections were overlaid using Lumina Vision software (Mitani, Tokyo, Japan) on a Power Macintosh G4 computer (Apple Computer, Cupertino, CA, USA).

### Electron microscopy

Small pieces of liver tissue were prefixed in 2.5% glutaraldehyde in 0.1 M phosphate buffer (PB, pH 7.4) for 24 h at 4°C and postfixed in 1% osmium tetroxide in PB for 2 h at 4°C followed by dehydration and embedding in epoxy resin. For selecting optimal areas, semithin sections were stained with toluidine blue. Ultrathin sections stained with uranyl acetate and lead citrate were examined with a JEM 100S electron microscope (JEOL, Tokyo, Japan).

### Statistical analysis

Peripheral blood CBC (complete blood count) and serum ALT and AST concentration were tested. Post hoc analysis by Fisher's protected least squares difference (PLSD) test was performed for comparison at different time points. All statistical calculations were made with a statistical software package (StatView II; Abacus Concepts, Berkeley, CA, USA). A value of $P < 0.05$ was considered to be statistically significant.

## Results

### Blood chemistry

The number of RBC ($\times 10^4$/μl) and the value of serum Hb (g/dl) showed no significant changes throughout the examination (Fig. 1). The number of WBC (/μl) showed the lowest level at 36 h and then gradually increased and returned to the normal level on day 14. Serum AST (IU/l) and ALT (IU/l) reached a peak at 36 h ($P < 0.001$) after DMN injection and then decreased with time.

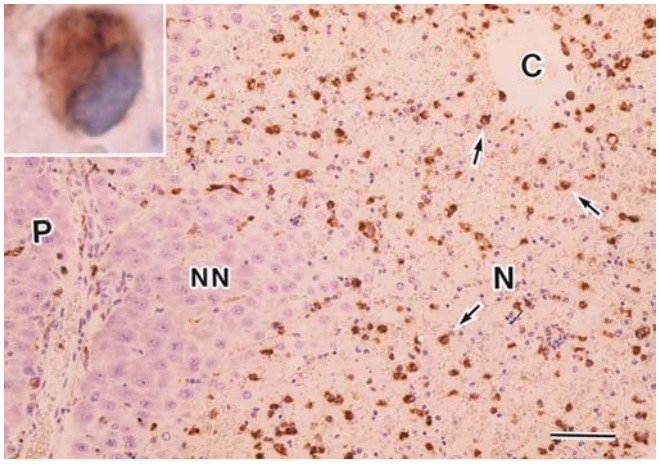


**Fig. 2.** Liver at 36 h after DMN injection. Numerous ED-1-positive large round mononuclear cells (*arrows*) infiltrate in necrotic areas. Immunohistochemical stain for ED-1. *Inset:* Higher magnification of an ED-1-positive round mononuclear cell. *C*, central vein; *N*, necrotic area; *NN*, nonnecrotic remaining liver parenchyma; *P*, portal tract. *Bar* 60 μm

## Light microscopic and immunohistochemical observations

In the control livers, inflammatory cell infiltrate was absent. Normal rat livers were negative for BrdU whereas a few BrdU-positive cells were detected in the normal rat bone marrow.

Liver tissues obtained from rats at the same period after DMN treatment showed similar morphological changes. Small focal necrosis appeared in liver lobules at 12 h after DMN injection. At 36 h, liver necrosis became most prominent. Various types of inflammatory cells, including macrophages, neutrophils, eosinophils, and lymphocytes, infiltrated in the necrotic areas. Among the inflammatory cells, large round (about 15 μm in diameter) mononuclear cells were predominant and positive for ED-1 (Fig. 2). On days 2 and 3 after injection, necrotic tissues and extravasated erythrocytes were phagocytosed by the ED-1-positive cells and gradually removed. On day 5, when most necrotic tissues were removed, the ED-1-positive round mononuclear cells were transformed to spindle-shaped cells with elongated cytoplasm (Fig. 3). These ED-1-positive spindle cells were attached to residual reticulin fibers (Fig. 3b). Some of the cells simultaneously showed a positive reaction for BrdU (Fig. 3c). The ED-1- and BrdU-positive cells appeared in the necrotic areas from day 2. On day 7, all ED-1-positive spindle cells were stained with iron.

On the other hand, numerous round-shaped ED-1-positive cells aggregated in the central vein (Fig. 4a). These cells showed a stronger intensity of iron staining compared with that of the spindle-shaped cells in necrotic areas on day 7 (Fig. 4b). On day 8, the findings of liver tissues were almost similar to those on day 7, except for the diminution of necrotic areas. Until day 0, regenerated liver trabeculae appeared and increased in volume in the necrotic area. In the perinecrotic areas, small islands of erythroblasts occurred after day 5. Most of them were strongly positive for BrdU. The erythroblastic islands increased in number and

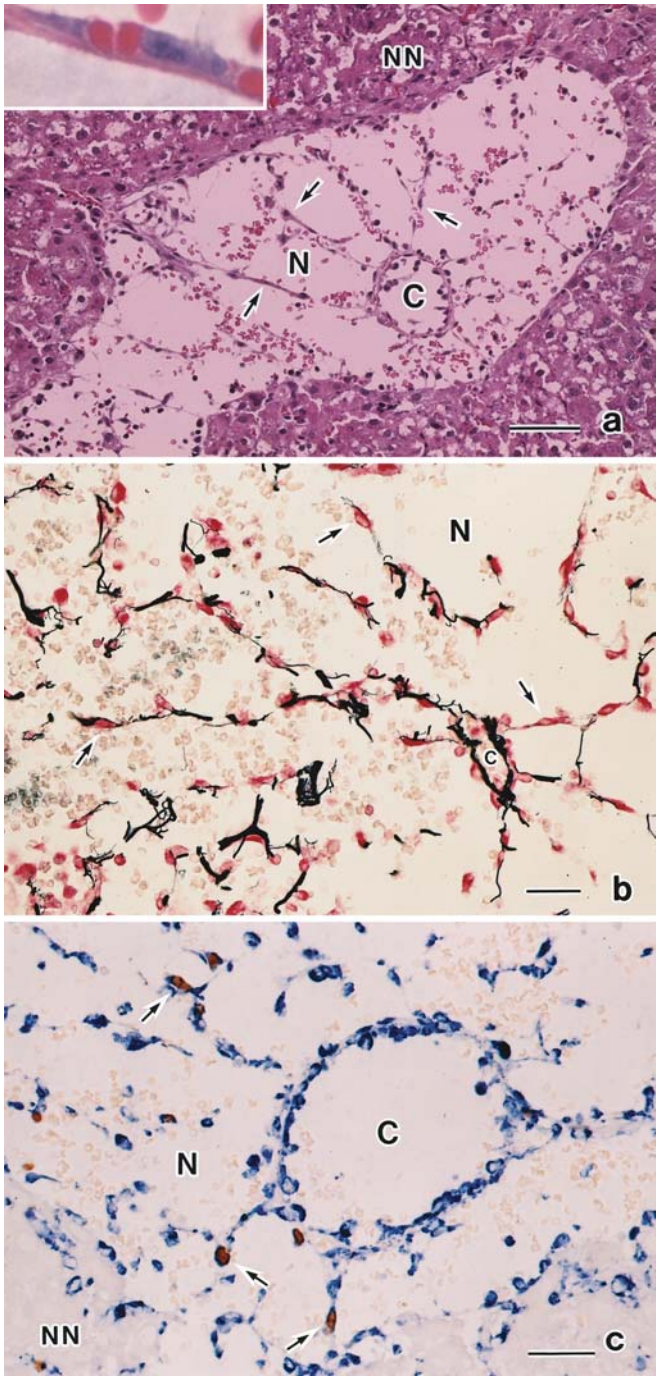


**Fig. 3a–c.** Liver on day 5 after DMN injection. **a** Most of the necrotic tissues are removed, leaving a punched-out-like lesion. An incomplete network of spindle cells (*arrows*) is formed in the necrotic area. Nonnecrotic remaining liver parenchyma still appears normal. The margin between necrotic areas and remaining liver parenchyma is sharp, and active sprouting of new blood vessels from the latter to necrotic areas appears to be absent. *Inset:* Higher magnification of a spindle cell showing avid erythrophagocytosis. Hematoxylin and eosin (H&E) stain. **b** The cytoplasm of the spindle cell stains *red* with ED-1; reticulin fibers stain *black*. The ED-1-positive spindle cells (*arrows*) are closely attached to reticulin fibers in the necrotic area. Silver impregnation and immunohistochemical stain for ED-1. **c** ED-1-positive spindle cells having a bromodeoxyuridine (BrdU)-labeled nucleus (*arrows*) are identified in the necrotic area. BrdU is stained *brown* and ED-1 is stained *blue*. Double immunohistochemical stain with anti-ED-1 and anti-BrdU antibodies. *C*, central vein; *N*, necrotic area; *NN*, nonnecrotic liver parenchyma. *Bars* **a** 60 μm; **b,c** 30 μm

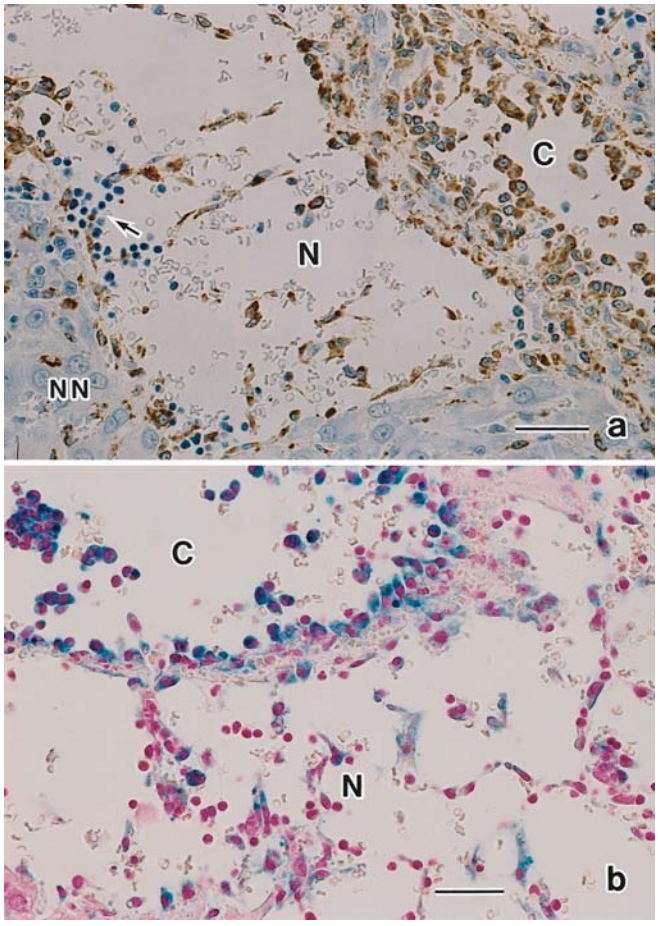


**Fig. 4a,b.** Liver on day 7 after DMN injection. **a** Both spindle cells in the necrotic area and round cells within a central vein show a positive reaction for ED-1. *Arrow* shows erythroblastic islands at the margin between the necrotic area and the nonnecrotic liver parenchyma. Immunohistochemical stain for ED-1. **b** Both the spindle and round cells are positive for iron stain (detected as *blue*). The iron staining is more intense in the round mononuclear cells gathered in the central vein, compared with the spindle cells in the necrotic areas. Iron stain. *C*, central vein; *N*, necrotic area; *NN*, nonnecrotic liver parenchyma. *Bars* **a** 60 μm; **b** 30 μm

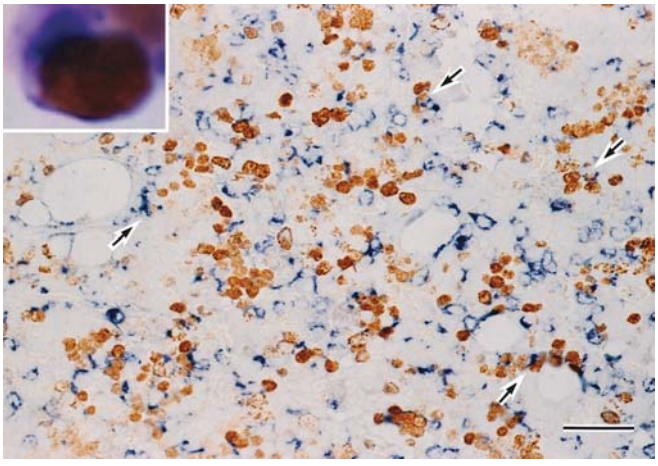

**Fig. 5.** Double immunohistochemical stain of bone marrow cells with ED-1 and BrdU at 36 h after DMN injection. Numerous BrdU (*brown*)-positive cells and ED-1 (*blue*)-positive cells are observed. Some of them are double positive for ED-1 and BrdU (*arrows*). *Inset*: Higher magnification of a double-positive mononuclear cell. *Bar* 30 μm

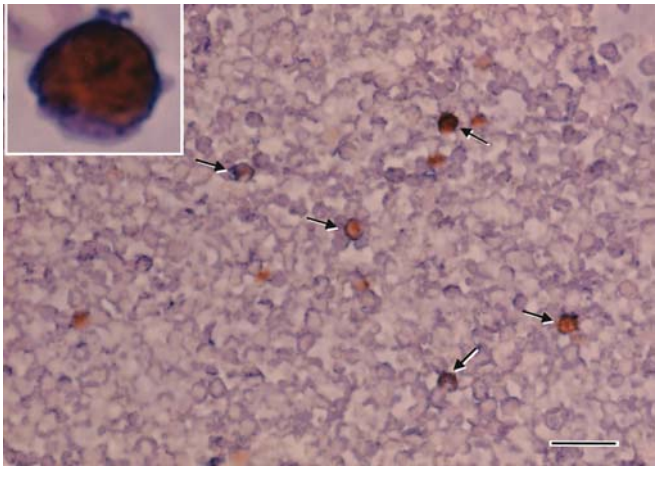

**Fig. 6.** Double immunohistochemical stain with ED-1 and BrdU of peripheral blood cells at 36 h after DMN injection. Numerous BrdU (*brown*)-positive cells and ED-1 (*blue*)-positive cells are observed. Double-positive cells for ED-1 and BrdU (*arrows*) are occasionally seen. *Inset*: Higher magnification of a double positive mononuclear cell for ED-1 and BrdU. *Bar* 30 μm

size to day 7 and disappeared by day 14 after DMN treatment. Necrotic tissue spaces were gradually replaced by regenerating liver parenchyma. On day 14, thin fibrous bands extended from adjoining centrilobular areas and connected with each other, resulting in the formation of thin, C–C (central-to-central) bridging fibrosis, as reported in our previous study.[21] The necrotic areas, which were significant in zones 2 and 3 from 36 h to day 5 after a DMN injection, were mostly replaced by regenerating liver parenchyma and partly by thin C–C bridging fibrosis, and almost disappeared. However, small necrotic foci were rarely seen scattered.

At 36 h, large round (about 10 μm in diameter) mononuclear cells showing the colocalization of ED-1 and BrdU were frequently observed in the bone marrow and peripheral blood. The ED-1 and BrdU double-positive cells were seen in the bone marrow from 12 h to day 7, having a peak at the period from 36 h to day 2 (Fig. 5), while they were observed in the peripheral blood from 24 h to day 10, having a peak at the period from 36 h to day 2 (Fig. 6).

The chronological changes of the numbers of single-positive cells for each ED-1 and SE-1, and double-positive cells for ED-1/BrdU or ED-1/SE-1, in bone marrow, peripheral blood, and necrotic and nonnecrotic liver tissues after DMN treatment are summarized in Table 2.

## Double immunofluoresecence staining for SE-1, and ED-1

Some of the ED-1-positive spindle cells in the necrotic area showed colocalization of SE-1 on day 7 (Fig. 7). Both ED-1-positive spindle cells in the necrotic area and round cells

**Table 2.** Occurence of single-positive cells for ED-1 and SE-1 and double-positive cells for ED-1/BrdU and ED-1/SE-1 in bone marrow, peripheral blood, and necrotic and nonnecrotic liver tissues at various time intervals after DMN treatment

| | 0 | 12 h | 24 h | 36 h | 2 d | 3 d | 5 d | 7 d | 10 d | 14 d |
|---|---|---|---|---|---|---|---|---|---|---|
| Bone marrow | | | | | | | | | | |
| ED-1 | + | + | ++ | +++ | +++ | ++ | ++ | ++ | + | + |
| ED-1/BrdU | – | + | ++ | +++ | +++ | ++ | ++ | + | – | – |
| ED-1/SE-1 | – | – | – | – | – | – | – | – | – | – |
| SE-1 | – | – | – | – | – | – | – | – | – | – |
| Periperal blood | | | | | | | | | | |
| ED-1 | + | + | ++ | +++ | +++ | ++ | ++ | +++ | +++ | ++ |
| ED-1/BrdU | – | – | + | ++ | ++ | + | + | + | + | – |
| ED-1/SE-1 | – | – | – | – | – | – | – | – | – | – |
| SE-1 | – | – | – | – | – | – | – | – | – | – |
| Liver (necrotic area) | | | | | | | | | | |
| ED-1 | | + | + | ++ | +++ | +++ | ++ | ++ | + | |
| ED-1/BrdU | | – | – | – | + | +++ | ++ | + | – | |
| ED-1/SE-1 | | – | – | – | – | + | + | ++ | + | |
| SE-1 | | – | – | – | – | + | + | ++ | + | |
| Liver (nonnecrotic) | | | | | | | | | | |
| ED-1 | ++ | ++ | ++ | + | + | + | ++ | ++ | ++ | +++ |
| ED-1/BrdU | – | – | – | + | ++ | +++ | ++ | + | – | – |
| ED-1/SE-1 | – | – | – | – | – | – | – | – | – | – |
| SE-1 | +++ | +++ | ++ | + | + | + | ++ | ++ | ++ | +++ |

d, day; BrdU, 5-bromo-2-deoxyuridine; DMN, dimetylnitrosamine; ED-1, antirat monocyte/macrophage; SE-1, antirat hepatic sinusoidal endothelial cell; –, none; +, a few; ++, moderate; +++, numerous

that aggregated in the central vein were simultaneously positive for Tie-1 at the same period (Fig. 8). At this period, HSEs in the remaining and regenerating liver tissues were positive for SE-1 or Tie-1 but did not stain for ED-1.

### Ultrastructural findings

After 36 h, not only liver parencymal cells but also hepatic sinusoidal endothelial cells (HSEs) and hepatic stellate cells (HSCs) showed marked degeneration and necrosis, and the intrinsic trabecular structure was completely lost. The vestige of previous sinusoids was scarcely discernible. Platelets and various types of inflammatory cells were observed in the necrotic area of DMN-treated rat livers (Fig. 9). On day 7, after removal of necrotic tissues, a primitive sinusoidal wall was developed, although liver parenchymal cells and HSC were still absent (Fig. 10a). In the reorganizing sinusoidal lumen and along the sinusoidal wall, round mononuclear cells and various transitional forms to spindle cells were seen (Fig. 10b–f). Some of the spindle cells showed various stages of erythrophagocytosis (Fig. 10a,d,e). Spindle cells were frequently attached to extracellular matrix components containing reticulin fibers on the abluminal surface of the cell (Fig. 10a,f). On day 8, in the regenerated tissue near the necrotic areas, spindle cells, which are very similar to sinusoidal endothelial cells, overlaid the hepatic cells and appeared to form a sinusoidal wall, although the Disse's space was not yet well reorganized (Fig. 11). A slightly dilated sinusoidal structure was detected in the regenerating parenchyma, which was more distant from the necrotic area. These sinusoidal endothelial cells had some fenestrated structure. HSCs were present in the well-developed Disse's space.

## Discussion

The ED-1- and BrdU-positive large round mononuclear cells infiltrated in the liver necrotic areas from day 2, while cells with the same cytological features were already seen as early as 12 h in the bone marrow and then at 24 h in the peripheral blood after DMN treatment. Previous studies reported that endothelial progenitor cells are derived from the bone marrow[3,11–16] and circulate in the peripheral blood of adult animals.[8–11,17] These findings suggest that the ED-1-positive large round mononuclear cells in necrotic liver areas are derived from the bone marrow. They may migrate to the necrotic area through the blood circulation. Ultrastructural examination showed an increase with time in the number of transitional cells, from large round mononuclear cells to spindle cells. From day 5, the spindle cells in necrotic areas showed a differentiation into HSEs, immunohistochemically confirmed by the expression of SE-1.

On the other hand, both spindle cells in the necrotic area and round cells in the central veins showed avid phagocytosis and positive reactions for ED-1, Tie-1, and iron staining. Namely, the bone marrow-derived ED-1-positive cells may differentiate to two types of cells, i.e., macrophages and HSEs. In the HSE lineage, the feature of phagocytosis may suggest a transition from the ED-1-positive large round mononuclear cells with phagocytotic activity to the SE-1-positive spindle HSEs or the phagocytosis of immature HSEs. Tie-1, the endothelial cell-specific receptor tyrosine kinase for angiopoietin, has been detected in vascular endothelial cells and some myeloid leukemia cells.[28–32] The gene is expressed in the early embryonic vascular system.[29] The angiopoietin/Tie signaling system is involved in the

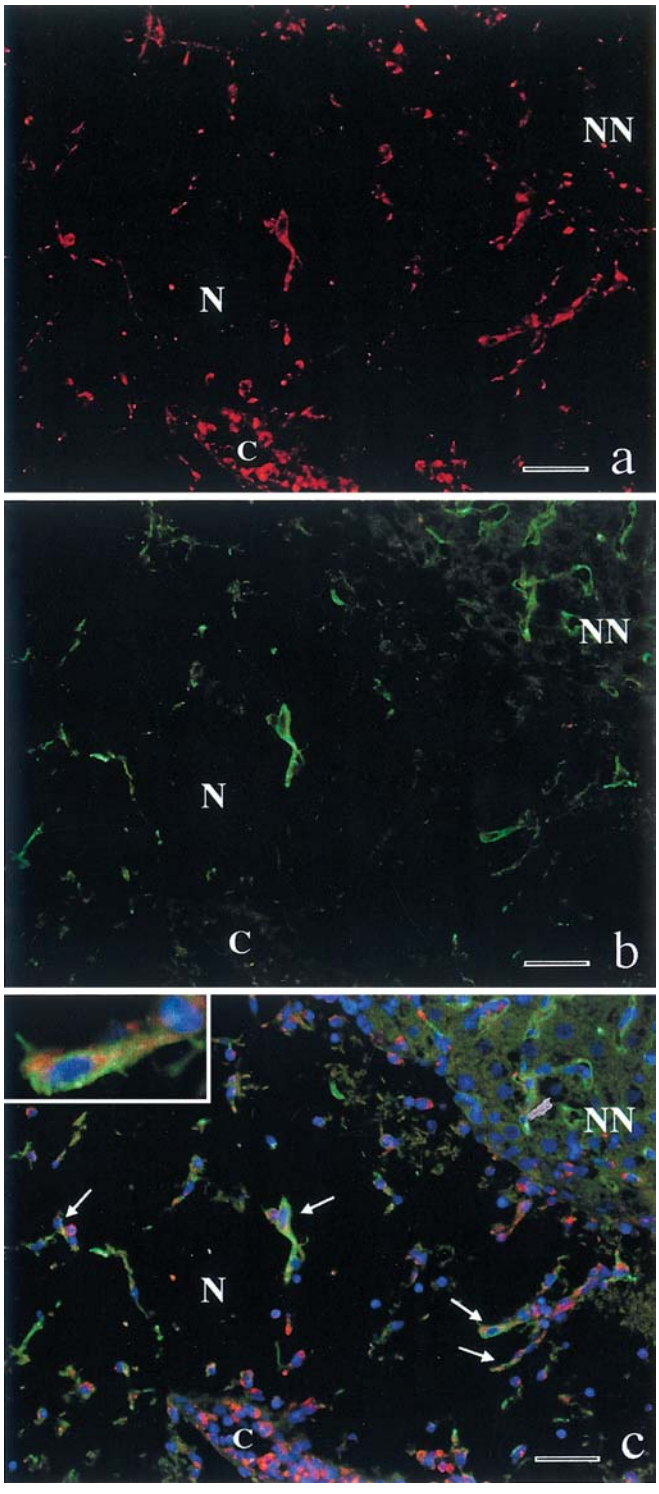


**Fig. 7a–c.** Double immunofluorescence for ED-1 and SE-1 in the liver on day 7 after DMN injection. **a** ED-1 (labeled with Alexa Fluor 594 mouse $IgG_1$) stained in *red*. **b** SE-1 [labeled with fluorescein isothiocyanate (FITC)] stained in *green*. **c** Double staining for ED-1 and SE-1. Some of the ED-1-positive mononuclear cells (*arrows*) are also positive for SE-1 in the necrotic area. Hepatic sinusoidal endothelial cells in nonnecrotic liver parenchyma are preferentially positive for SE-1. Nucleus showed *blue* color with TAPI. *Inset*: Higher magnification of a double-positive cell for ED-1 and SE-1. *C*, central vein; *N*, necrotic area; *NN*, nonnecrotic liver parenchyma. *Bars* 30 μm

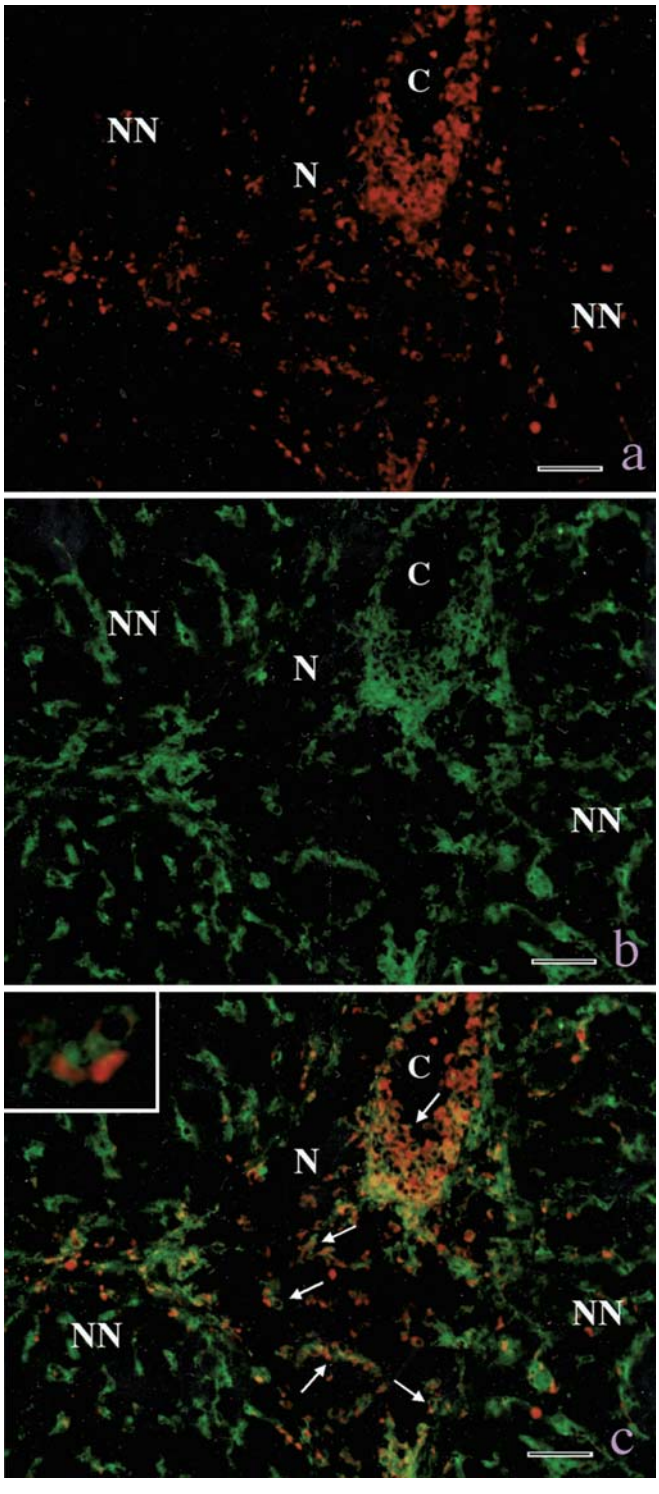


**Fig. 8a–c.** Double immunofluorescence for ED-1 and Tie-1 in the liver on day 7 after DMN injection. **a** ED-1 (labeled with Alexa Fluor 594 mouse $IgG_1$) stained in *red*. **b** Tie-1 (labeled with FITC) stained in *green*. **c** Double staining for ED-1 and Tie-1. Some of the ED-1-positive mononuclear cells (*arrows*) are also positive for Tie-1 in the necrotic area. Hepatic sinusoidal endothelial cells (HSEs) in nonnecrotic liver parenchyma are preferentially positive for Tie-1. *Inset:* Higher magnification of a double-positive cell for ED-1 and Tie-1. *C*, central vein; *N*, necrotic area; *NN*, nonnecrotic liver parenchyma. *Bar* 30 μm

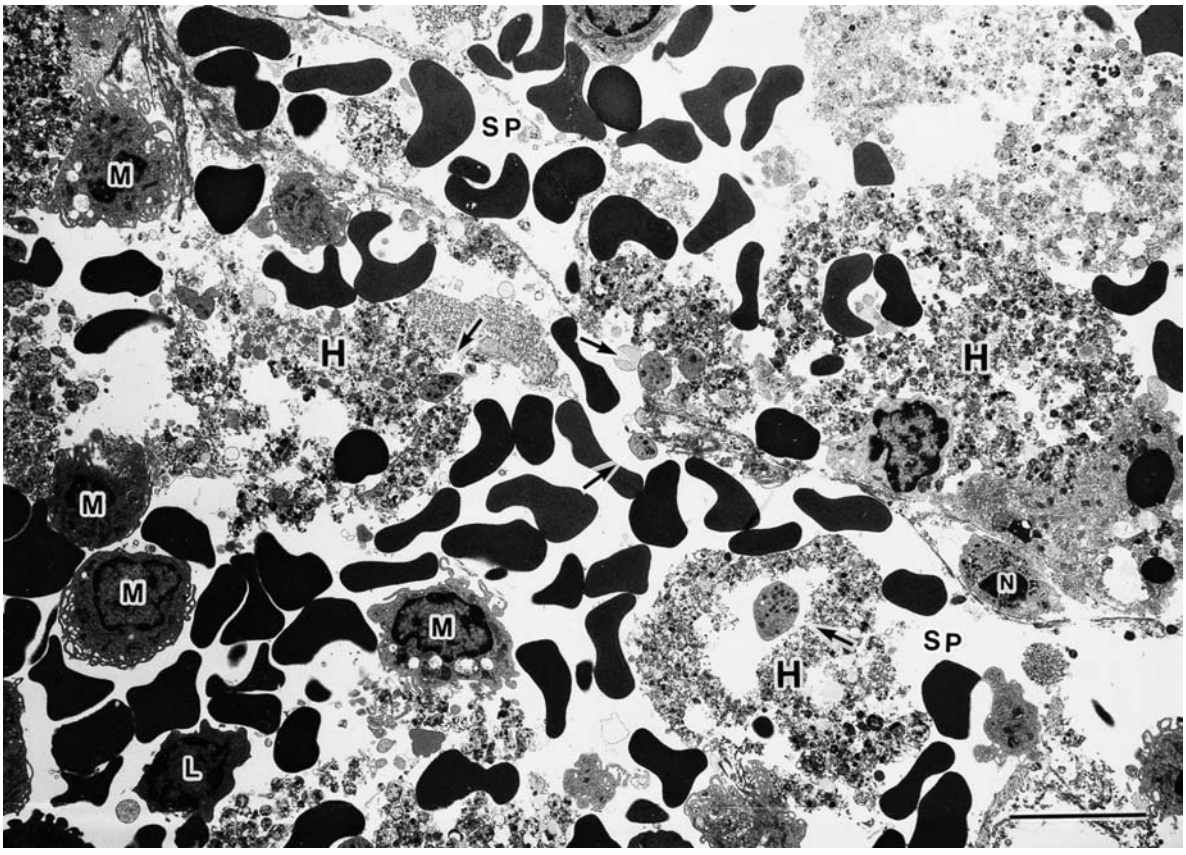


**Fig. 9.** A necrotic area at 36h after DMN injection. Numerous inflammatory cells consisting of mononuclear cells/macrophages (*M*), a neutrophil (*N*), and a lymphocyte (*L*) and platelets (*arrows*) are identified. The trabecular arrangement of liver cells and sinusoidal structure is almost completely lost. HSEs and even hepatic stellate cells are not present. *H*, necrotic hepatocyte; *SP*, scarcely discernible sinusoidal structure. *Bar* 10μm

secondary stages of vessel growth; vessel remodeling, maturation, and formation of complex hierarchical networks.[32] Sato et al.[33] reported that the Tie-1 knockout mice died before embryonic day 15 or immediately after birth (depending on the genetic background). The cause of death was considered to be the loss of microvascular integrity, resulting in severe hemorrhage.[31,33,34]

Tie-1 receptor tyrosine kinase may evolve for multiple protein–protein interaction, possibly including cell adhesion to the vascular endothelium.[28] In the present study, both ED-1-positive spindle cells in the necrotic area and round cells aggregated in the central vein were also positive for Tie-1, suggesting the same stem cell origin of these cells. In the liver parenchyma adjacent to the necrotic areas, erythroblastic islands increased in number with a peak from day 5 to day 7 and had a high proliferative activity. However, Hb and RBC level showed no significant changes, compared with the control group. Flamme and Risau[35] reported a similar phenomenon in an in vitro study. Cells used for culture in their study were from blastodiscs of stages X to XII from unincubated quail egges. As a result, the cell islands were composed of both round erythropoietic cells at the center and spindle-shaped endothelial cells at the periphery of the cell cultures after 3 days under treatment with basic fibroblast growth factor.[35] Together with consideration of their results, the ED-1-positive stem cells may differentiate not only to macrophages and HSEs but also to erythroblasts in perinecrotic zones.

According to previous studies, hepatic stellate cells (HSCs) survive even in severe parenchymal necrosis[36] and significant destruction of lobular architecture.[37] They are activated and play a significant role in postnecrotic liver remodeling[36,38] and biliary fibrosis, resulting in obstruction of the common bile duct.[37] However, following a single large-dose injection of DMN, all types of cells in zones 2 and 3 including HSCs fell into complete necrosis.[21] In the necrotic area, along the vestige of previous sinusoids, small fragments of degenerated and necrotic endothelial cells and small amounts of collagen fibrils are only scattered. Hepatic stellate cells are lost. Then, numerous ED-1-positive mononuclear cells attach to residual reticulin fibers and contribute to tissue remodeling instead of necrotic HSCs. The restoration of HSEs in the necrotic area may be predominantly accomplished by the infiltrated ED-1-positive cells, namely by vasculogenesis rather than by angiogenesis. Shintani et al.[39] reported that cultured rabbit bone marrow mononuclear cells changed to spindle-shaped cells and began to sprout from the edge of the cell clusters within 3 days

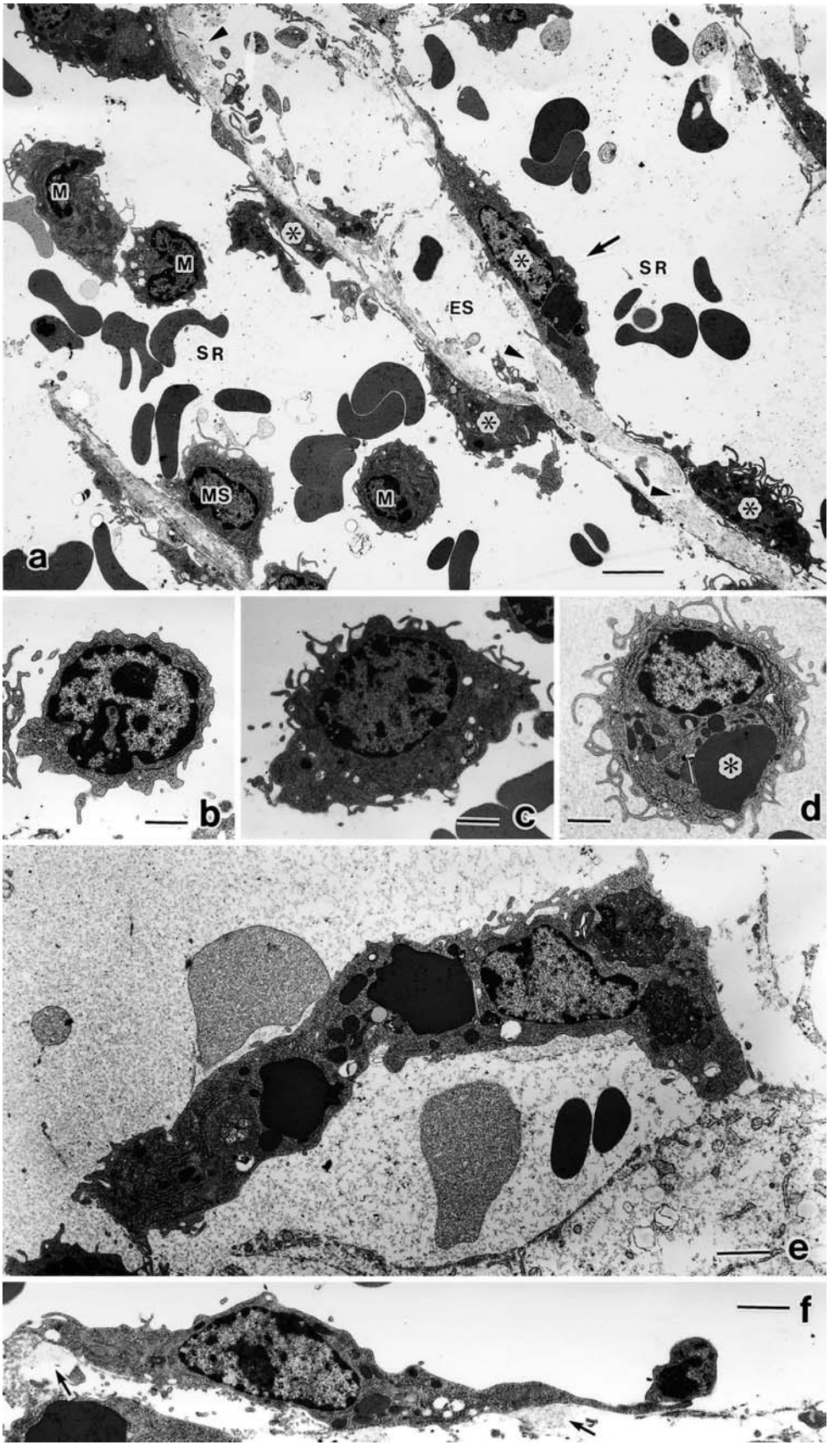


**Fig. 10a–f.** Round to spindle cells in the necrotic area on day 7 after DMN injection. **a** Mononuclear cells/macrophages (*M*) are predominantly seen and mainly located in the lumen of reorganizing sinusoid (*SR*), whereas a few of them are attached to the sinusoidal wall. Elongated spindle cells (*) attached to the residual reticulin fibers (*arrowheads*) contain phagocytosed materials. The round cells marked as *MS* attach to the putative sinusoidal wall. The extrasinusoidal portion (*ES*) is composed of loose extracellular matrix. Hepatocytes and hepatic stellate cells are not yet seen. *SR*, reorganizing sinusoid. **b–f** Cells in various stages of transition from round mononuclear cells to spindle cells in necrotic areas. **b** A round mononuclear cell with a high nuclear cytoplasmic ratio shows a large round nucleus with a prominent nucleolus, without any features of differentiation and any signs of phagocytosis. In scanty cytoplasm numerous polyribosomes are present. Short fragments of rough-surfaced endoplasmic reticulum are scattered. **c** A short filopodia and a few vacuoles and small secondary lysosomes are seen. **d** A mononuclear cell shows erythrophagocytosis (*) and well-developed filopodia. **e** A spindle-shaped cell with avid phagocytosis. **f** A spindle-shaped cell closely attached to residual reticulin fibers (*arrows*) has a few dense bodies in the cytoplasm. Slender cytoplasmic processes are extended. *Bars* **a** 5 μm; **b–f** 1.8 μm

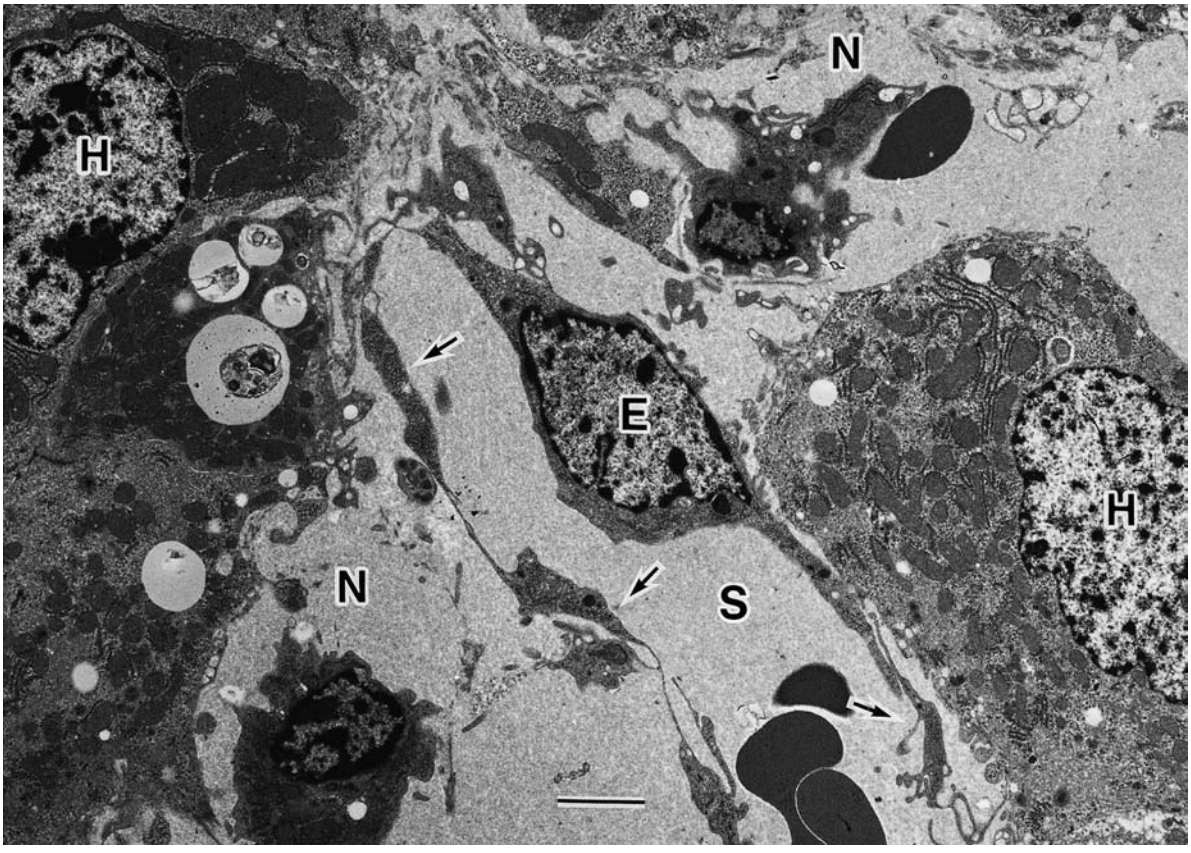


**Fig. 11.** At day 8, a sinusoidal endothelial-like cell (*E*) with an elongated cytoplasm partly surrounds a hepatic cell (*H*) in the newly regenerating tissue adjacent to the necrotic area (*N*). The sinusoidal endothelial cell forms a sinusoid-like structure (*S*) with other endothelial-like cells (*arrows*). *Bar* 2.5 μm

and formed a network of spindle cells. After day 7 of culture, the spindle cells became positive for both *Ulex* europaeus lectin binding and von Willebrand factor (vWF), which are characteristic markers for endothelial cell lineage.[39]

Newly formed sinusoids in the necrotic areas, as shown in Figs. 10 and 11, are slightly dilated. The cytoplasm of sinusoidal endothelial cells is elongated, but with no degenerative changes. With further development of sinusoids, the endothelial cells show thin fenestrated cytoplasm. In the space of Disse between regenerating liver parenchymal cells and sinusoidal endothelial cells, the hepatic stellate cells are present. However, to demonstrate more clearly the capacity of bone marrow cells (BMC) to differentiate into sinusoidal endothelial cells in the hepatic necrotic areas, it may be necessary, for example, to inject intravenously the BMC labeled with fluorescent protein into the rats and show the appearance of the labeled BMC and the differentiation to sinusoidal endothelial cells in the injured areas.

In conclusion, our results from morphological observations at various time intervals after DMN treatment suggest that the infiltrating ED-1 and BrdU-positive round and large mononuclear cells in the necrotic area may be derived from the bone marrow. They may proliferate and ultimately differentiate to SE-1-positive HSEs and regenerate the sinusoidal structure, showing vasculogenesis. Furthermore, in addition to HSEs, macrophages in necrotic areas and erythropoietic cells in perinecrotic areas may have the same origin. Because this rat model for submassive complete necrosis induced by a DMN injection is highly stable and reproducible, it may be useful in understanding the mechanisms and factors involved in the vasculogenesis of adult livers.

**Acknowledgments** We thank Mr. T. Tokaji, Ms. H. Yamasaki, Ms. T. Kadota, and Ms. Y. Tanaka, Department of Pathology, and Mr. M. Shirota, Medical Research Laboratory, Kochi Medical School, for their excellent technical assistance. We are also grateful to Mr. D. Ribble and J.D. Hare, Department of English, Kochi Medical School, for English correction of our manuscript. This study was supported by a Grant-in-Aid for Scientific Research from the Ministry of Education, Culture, Sports, Science and Technology (MEXT) in Japan, grant C 13670176.

## References

1. Folkman J, Shing Y (1992) Angiogenesis. J Biol Chem 267:10931–10934
2. Asahara T, Murohara T, Sullivan A, Silver M, Zee RVD, Li T (1997) Isolation of putative progenitor endothelial cells for angiogenesis. Science 275:964–967
3. Asahara T, Masuda H, Takahashi T, Kalka C, Pastore C, Silver M, Kearne M, Magner M, Isner JM (1999) Bone marrow origin of

endothelial progenitor cells responsible for postnatal vasculogenesis in physiological and pathological neovascularization. Circ Res 85:221–228
4. Risau W, Sariola H, Zerwes HG, Sasse J, Ekblom P, Kemler R, Doetschman T (1988) Vasculogenesis and angiogenesis in embryonic-stem-cell-derived embryoid bodies. Development (Camb) 102:471–478
5. Risau W (1991) Embryonic angiogenesis factors. Pharmacol Ther 51:371–376
6. Risau W, Flamme I (1995) Vasculogenesis. Annu Rev Cell Dev Biol 11:73–91
7. Arcalis T, Carretero A, Navarro M, Ayuso E, Ruberte J (2002) Vasculogenesis and angiogenesis in the subcardinal venous plexus of quail mesonephros: spatial and temporal morphological analysis. Anat Embryol 205:19–28
8. Kalka C, Masuda H, Takahashi T, Gordon R, Tepper O, Gravereaux E, Pieczek A, Iwaguro H, Hayashi SI, Isner JM, Asahara T (2000) Vascular endothelial growth factor$_{165}$ gene transfer augments circulating endothelial progenitor cells in human subjects. Circ Res 86:1198–1202
9. Moldovan NI, Goldschmidt-Clermont PJ, Parker-Thornburg J, Shapiro SD, Kolattukudy PE (2000) Contribution of monocytes/macrophages to compensatory neovascularization. The drilling of metalloelastase-positive tunnels in ischemic myocardium. Circ Res 87:378–384
10. Murohara T, Ikeda H, Duan J, Shintani S, Sasaki KI, Eguchi H, Onitsuka I, Matsui K, Imaizumi T (2000) Transplanted cord blood-derived endothelial precursor cells augment postnatal neovascularization. J Clin Invest 105:1527–1536
11. Nabel EG (2002) Stem cells combined with gene transfer for therapeutic vasculogenesis: magic bullets? Circulation 105:672
12. Shi Q, Rafii S, Wu MHD, Wijelath ES, Yu C, Ishida A, Fujita Y, Kothari S, Mohle R, Sauvage LR, Moore MAS, Storb RF, Hammond WP (1998) Evidence for circulating bone marrow-derived endothelial cells. Blood 92:362–367
13. Takahashi T, Kalka C, Masuda H, Chen D, Silver M, Kearney M, Magner M, Isner JM, Asahara T (1999) Ischemia-and cytokine-induced mobilization of bone marrow-derived endothelial progenitor cells for neovascularization. Nat Med 5:434–438
14. Gunsilius E, Duba HC, Petzer AL, Kähler CM, Grünewald K, Stockhammer G, Gabl C, Dirnhofer S, Clausen J, Gastl G (2000) Evidence from a leukaemia model for maintenance of vascular endothelium by bone-marrow-derived endothelial cells. Lancet 355:1688–1691
15. Llevadot J, Murasawa S, Kureishi Y, Uchida S, Masuda H, Kawamoto A, Walsh K, Isner JM, Asahara T (2001) HMG-CoA reductase inhibitor mobilizes bone marrow-derived endothelial progenitor cells. J Clin Invest 108:399–405
16. Zhang ZG, Zhang L, Jiang Q, Chopp M (2002) Bone marrow-derived endothelial progenitor cells participate in cerebral neovascularization after focal cerebral ischemia in the adult mouse. Circ Res 90:284–288
17. Rafii S (2000) Circulating endothelial precursors: mystery, reality, and promise. J Clin Invest 105:17–19
18. Enomoto K, Nishikawa Y, Omori Y, Tokairin T, Yoshida M, Ohi N, Nishimura T, Yamamoto Y, Li Q (2004) Cell biology and pathology of liver sinusoidal endothelial cells. Med Electron Microsc 37:208–215
19. Wisse E, Braet F, Luo D, Vermijlen D, Eddouks M, Konstandoulaki M, Empsen C, Zanger RBD (1999) Endothelial cells of the hepatic sinusoids: a review. In: Tanikawa K, Ueno T (eds) Liver diseases and hepatic sinusoidal cells. Springer, Tokyo, pp 17–55
20. Deleve LD, Shulman HM, McDonald GB (2002) Toxic injury to hepatic sinusoids: sinusoidal obstruction syndrome (veno-occlusive disease). Semin Liver Dis 22:27–42
21. Jin YL, Enzan H, Kuroda N, Hayashi Y, Nakayama H, Zhang YH, Toi M, Miyazaki E, Hiroi M, Guo LM, Saibara T (2003) Tissue remodelling following submassive hemorrhagic necrosis in rat livers induced by an intraperitoneal injection of dimethylnitrosamine. Virchows Arch 442:39–47
22. Yee SB, Hanumegowda UM, Copple BL, Shibuya M, Ganey PE, Roth RA (2003) Endothelial cell injury and coagulation system activation during synergistic hepatotoxicity from monocrotaline and bacterial lipopolysaccharide coexposure. Toxicol Sci 74:203–214
23. Ray SD, Sorge CL, Kamendulis LM, Corcoran GB (1992) $Ca^{++}$-activated DNA fragmentation and dimethylnitrosamine-induced hepatic necrosis: Effects of $Ca^{++}$-endonuclease and poly (ADP-ribose) polymerase inhibitors in mice. J Pharmacol Exp Ther 263:387–394
24. Oyaizu T, Shikata N, Senzaki H, Matsuzawa A, Tsubura A (1997) Studies on the mechanism of dimethylnitrosamine-induced acute liver injury in mice. Exp Toxicol Pathol 49:375–380
25. Bussolati G (1982) A celloidin bag for the histological preparation of cytologic material. J Clin Pathol 35:574–576
26: Ohmura T, Enomoto K, Satoh H, Sawada N, Mori M (1993) Establishment of a novel monoclonal antibody, SE-1, which specifically reacts with rat hepatic sinusoidal cells. J Histochem Cytochem 41:1253–1257
27. Hines JE, Johnson SJ, Burt AD (1993) *In vivo* responses of macrophages and perisinusoidal cells to cholestatic liver injury. Am J Pathol 142:511–518
28. Partanen J, Armstrong E, Mäkelä TP, Korhonen J, Sandberg M, Renkonen R, Knuutila S, Huebner K, Alitalo K (1992) A novel endothelial cell surface receptor tyrosine kinase with extracellular epidermal growth factor homology domain. Mol Cell Biol 12:1698–1707
29. Sato TN, Qin Y, Kozak CA, Audus KL (1993) *tie-1* and *tie-2* define another class of putative receptor tyrosine kinase genes expressed in early embryonic vascular system. Proc Natl Acad Sci USA 90:9355–9358
30. Partanen J, Dumont DJ (1999) Functions of Tie1 and Tie2 receptor tyrosine kinases in vascular development. Curr Top Microbiol Immunol 237:159–172
31. Tallquist MD, Soriano P, Klinghoffer RA (1999) Growth factor signaling pathways in vascular development. Oncogene 18:7917–7932
32. Thurston G (2003) Role of angiopoietins and Tie receptor tyrosine kinases in angiogenesis and lymphangiogenesis. Cell Tissue Res 314:61–68
33. Sato TN, Tozawa Y, Deutsch U, Wolburg-Buchholz K, Fujiwara Y, Gendron-Maguire M, Gridley T, Wolburg H, Risau W, Qin Y (1995) Distinct roles of the receptor tyrosine kinases Tie-1 and Tie-2 in blood vessel formation. Nature (Lond) 376:70–74
34. Puri MC, Rossant J, Alitalo K, Bernstein A, Partanen J (1995) The receptor tyrosine kinase TIE is required for integrity and survival of vascular endothelial cells. EMBO J 14:5884–5891
35. Flamme I, Risau W (1992) Induction of vasculogenesis and hematopoiesis *in vitro*. Development (Camb) 116:435–439
36. Enzan H, Himeno H, Iwamura S, Saibara T, Onishi S, Yamamoto Y, Miyazaki E, Hara H (1995) Sequential changes in human Ito cells and their relation to postnecrotic liver fibrosis in massive and submassive hepatic necrosis. Virchows Arch 426:95–101
37. Tao LH, Enzan H, Hayashi Y, Miyazaki E, Saibara T, Hiroi M, Toi M, Kuroda N, Naruse K, Jin YL, Guo LM (2002) Appearance of denuded hepatic stellate cells and their subsequent myofibroblast-like transformation during the early stage of biliary fibrosis in the rat. Med Electron Microsc 33:217–230
38. Gressner AM (1996) Transdifferentiation of hepatic stellate cells (Ito cells) to myofibroblasts: a key event in hepatic fibrogenesis. Kidney Int Suppl 54:S39–S45
39. Shintani S, Murohara T, Ikeda H, Ueno T, Sasaki KI, Duan J, Imaizumi T (2001) Augmentation of postnatal neovascularization with autologous bone marrow transplantation. Circulation 103: 897–903